Colloids and Surfaces B: Biointerfaces 143 (2016) 111–117

Contents lists available at ScienceDirect

Colloids and Surfaces B: Biointerfaces

journal homepage: www.elsevier.com/locate/colsurfb

Biocompatibility and degradation of gold-covered magneto-elastic biosensors exposed to cell culture

C. Menti[a], M. Beltrami[b], A.L. Possan[b], S.T. Martins[a], J.A.P. Henriques[a], A.D. Santos[c], F.P. Missell[b], M. Roesch-Ely[a,*]

[a] Laboratório de Genômica, Proteômica e Reparo de DNA, Instituto de Biotecnologia, Universidade de Caxias do Sul, Brazil
[b] Laboratório de Caracterização Magnética, CCET, Universidade de Caxias do Sul, Brazil
[c] Instituto de Física, Universidade de São Paulo, São Paulo, SP, Brazil

ARTICLE INFO

Article history:
Received 4 December 2015
Received in revised form 17 February 2016
Accepted 10 March 2016
Available online 14 March 2016

Keywords:
Biocompatibility
CHO cells
Magneto-elastic alloy
Au-coating
MTT assay
AO/EB staining
ICP-OES

ABSTRACT

Magneto-elastic materials (ME) have important advantages when applied as biosensors due to the possibility of wireless monitoring. Commercial Metglas 2826MB3™ (FeNiMoB) is widely used, however sensor stabilization is an important factor for biosensor performance. This study compared the effects of biocompatibility and degradation of the Metglas 2826MB3™ alloy, covered or not with a gold layer, when in contact with cell culture medium. Strips of amorphous Metglas 2826MB3™ were cut and coated with thin layers of Cr and Au, as verified by Rutherford Backscattering Spectroscopy (RBS). Using Inductively Coupled Plasma-Optical Emission Spectrometry (ICP-OES), the presence of metals in the culture medium was quantitatively determined for up to seven days after alloy exposure. Biocompatibility of fibroblast Chinese Hamster Ovary (CHO) cultures was tested and cytotoxicity parameters were investigated by indirect means of reduction of MTT (3-(4,5-dimethylthiazol-2-yl)-2,5-diphenyltetrazolium bromide) at 1, 2 and 7 days. Cell death was further evaluated through *in situ* analysis using Acridine Orange/Ethidium Bromide (AO/EB) staining and images were processed with ImageJ software. Ions from Metglas® 2826MB3™ induced a degradation process in living organisms. The cytotoxicity assay showed a decrease in the percentage of live cells compared to control for the ME strip not coated with gold. AO/EB *in situ* staining revealed that most of the cells grown on top of the gold-covered sensor presented a normal morphology (85.46%). Covering ME sensors with a gold coating improved their effectiveness by generating protection of the transducer by reducing the release of ions and promoting a significant cell survival.

1. Introduction

Magneto-elastic (ME) sensors [1,2] have attracted considerable interest within the sensor community as an excellent platform for measuring a wide range of chemical and biological parameters. From the detection of hydrocarbons [3] to the determination of glucose in urine sample [4] to the evaluation of contaminants in milk [5,6], ME sensors have proven their usefulness. ME materials have advantages when applied as biosensors in the biomedical area due to the possibility of wireless monitoring [7,8]. Amorphous ME ribbons have been widely used in various studies, including determined efforts to detect food contaminants [9,10]. They have also been used in several applications, like monitoring growth in cell cultures [11], evaluating cell behavior such as adhesion [12] and controlling restenosis in peripheral artery stents [13].

The application of magnetic materials in biological problems naturally leads to the question of the compatibility of the magnetic material with the biological system under consideration. Magnetic materials in the form of nanoparticles [14,15] or thin films [16] have recently been examined from the point of view of possible toxic or injurious effects which might be caused. This is a more restricted form of biocompatibility and does not contemplate any positive interactions between biological tissues and the magnetic materials.

The ME amorphous alloy Metglas® 2826MB™, for example, is readily available for use in the development of biomedical devices, but requires special care, since ion release can promote cell cytotoxicity [12,17]. That alloy has approximate composition $Fe_{45}Ni_{45}Mo_3B_7$ and molybdenum and nickel are reported to have harmful effects on organisms. Molybdenum has been associated with various toxic effects on the body, causing damage to various

* Corresponding author at: Universidade de Caxias do Sul, Rua Francisco Getúlio Vargas 1130, 95070-560 Caxias do Sul, RS, Brazil.
E-mail address: mrely@ucs.br (M. Roesch-Ely).

http://dx.doi.org/10.1016/j.colsurfb.2016.03.034
0927-7765/

organs such as kidney, liver and spleen [18,19]. Nickel is known to be carcinogenic and toxic [20]. The dose-dependent cytotoxic effect of nickel has been reported in cultured fibroblasts [21]. A recent study showed that molybdenum nanoparticles (Mo-NPs) induced cytotoxicity in mouse skin fibroblast cells (L929), with decrease in cell viability and alterations in cell morphology [22]. The search for coatings that promote biocompatibility and stability in ME alloys for biological systems has been recently reported [17]. However, the performance of a biosensor for the wireless monitoring of biological samples can be affected by the application of these coatings. Different types of analyte solutions, such as the ones based on buffered salt solutions, which preserve living organisms, can induce accelerated corrosion of the magneto-elastic material and the release of toxic ions. The coating of these materials with nanometric chrome and gold films provides a surface capable of immobilizing the bioactive component. In addition, the preservation of the physical and mechanical properties of these sensors [23] has been attributed to the presence of a gold coating.

In order to investigate cytotoxic effects of ions in cell cultures, this study considered the effects of biocompatibility and degradation of the Metglas® 2826MB3™ alloy, as well as the effects of a gold covering layer, when in contact with cell culture medium. Cell cytotoxicity was evaluated through MTT, which measures the reduction of MTT (3-(4,5-dimethylthiazol-2-yl)-2,5-diphenyltetrazolium bromide) according to the methodology described by Denizolt and Lang [24]. Cell death induction was further evaluated through Acridine Orange/Ethidium Bromide (AO/EB) staining. Finally a quantitative determination of the presence of metal ions in the cell culture medium was made. This allowed an evaluation of the beneficial effects of the presence of a gold covering layer on the ME material. It also allows us to determine the time scale for these effects.

2. Material and methods

2.1. Substrate preparation

The amorphous alloy Metglas® 2826MB3™ was supplied by the Metglas Corp. of Conway SC, with approximate composition in wt.% of $Fe_{45}Ni_{45}Mo_3B_7$. The alloy was supplied in the form of 2 in. wide ribbons. The ribbons were first mechanically polished on both sides using a Struers Tegramin 20 polishing system with 0.05 μm alumina and water. After 1.5 h of polishing, their thickness was reduced to about ~15 μm. The debris or grease retained from the polishing process was removed by cleaning the strips ultrasonically in 100% methanol for 30 min. After the cleaning process, tapes were sputtered-coated (AJA, model ATC 2000) on both sides with a protective layer of chromium and then with gold. The Au-coated strips were cut to dimensions 5 mm × 1 mm × 15 μm. Bare alloy strips were cut to dimensions 5 mm × 1 mm × 30 μm with a microdicing saw. ME ribbons were sterilized at 200 °C for 120 min before exposure to cell culture medium.

2.2. Substrate characterization

The thicknesses of the chromium and gold layers were evaluated by Rutherford Backscattering Spectroscopy (RBS). Simulations of the spectra associated with deposited layers were made with the usual RUMP software routines [25,26]. The covered sensor surfaces were examined using Scanning Electron Microscopy (SEM).

2.3. Cell culture

Chinese Hamster Ovary cell lines were purchased from American Type Culture Collection (CCL-61, ATCC). Cells were cultured in Dulbeccoís Modified Eagleís Medium (DMEM), supplemented with 10% of Fetal Bovine Serum (FBS) and 1% of penicillin-streptomycin BRL; Life Technologies (Van Allen Way, Carlsbad, CA, USA). Cell lines were kept in a humidified atmosphere at 37 °C and 5% of CO_2.

2.4. Cytotoxicity assay

Cell cytotoxicity was assessed through MTT, an indirect cytotoxic test based on the formation and colorimetric quantification of an enzyme reaction product, which evaluates the reduction of MTT (3-(4,5-dimethylthiazol-2-yl)-2,5-diphenyltetrazolium bromide) according to the methodology described by Denizolt and Lang [24]. Briefly, 8×10^4 cells were inoculated for analysis after one day, 10^3 cells for analysis after two days, and 5×10^2 cells after seven days exposure to the strip surface. Afterward cells were seeded with 1 mL of supplemented culture medium in a 24-well plate and incubated for 24 h at 37 °C. The ME alloy was placed in the well for different incubation times (1, 2 and 7 days), while the solution of MTT (1 mg/mL in serum-free medium) was added for two hours after the incubation period. The formazan crystals were dissolved with dimethyl sulfoxide (DMSO) for 30 min, and the absorbance was measured using a microplate reader (Spectra Max M2e, Molecular Devices) at 570 nm. The absorbance of the negative control (cells without ME alloy) represents 100%. The percentage of growth inhibition was calculated as: cell viability (%) = (absorbance of experimental wells/absorbance control wells) × 100. Each experiment was performed in triplicate.

2.5. Acridine Orange/Ethidium Bromide (AO/EB) staining and image processing

The AO/EB technique is suitable to visualize viable cells and cell death induction. Initially, 8×10^4 cells/well were seeded in 24 well plates and incubated for 24 h with bare or Au-covered magneto-elastic strips. After incubation, the strips were washed twice with phosphate buffer saline (PBS). Cell death was evaluated through a direct *in situ* analysis on the surface of the sensor using Ethidium Bromide and Acridine Orange (Sigma-Aldrich). Each surface received 2 μL of AO and EB (100 μg/mL). Images were taken with a fluorescent light microscope (BX43—Olympus) with 10× and 40× objective magnification. The correlation between the intensity of green and red pixels were analyzed using ImageJ software v. 1.50 (http://rsb.info.nih.gov) and processed as described by Mironova et al. [27]. Briefly, AO/EB images were divided into three channels (R-red, G-green, B-black). Images of the green and red channels were quantified and the correlation plot of co-localized and non colocalized fluorescence was processed. Non-correlated pixels looked green and red and were attributed to living and dead cells, respectively. Correlated pixels looked yellow-orange and were also attributed to dead cells. The percentage of live cells was determined by dividing the number of green pixels by the total number of red and green pixels. The threshold was fixed at an intensity of 75, determined by the 8 bits extraction of channel images.

2.6. Ions concentration in media culture

To evaluate ion detachment into the medium from the surface of ME strips not covered with Au, the strips were placed in 160 mL of DMEM. After 7 days, the strips were removed and weighed dry. The incubation medium was sent for analysis by Inductively Coupled Plasma-Optical Emission Spectrometry (ICP-OES) method. Analysis was performed by the laboratory *Greenlab® Análises químicas e toxicológicas Ltda.*

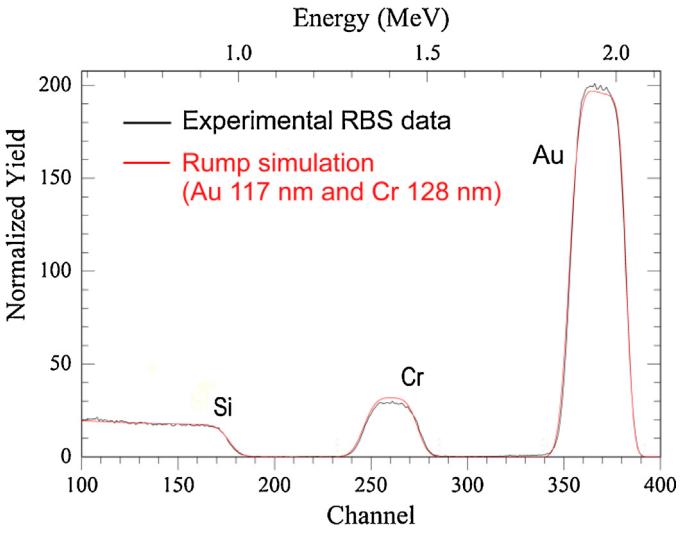

Fig. 1. Rutherford backscattering spectrum (RBS) for layers of Cr and Au on a Si substrate, with the simulated spectrum, taken from Ref. [30]. The simulation assumed a Cr layer of 128 nm as well as a Au layer of 117 nm.

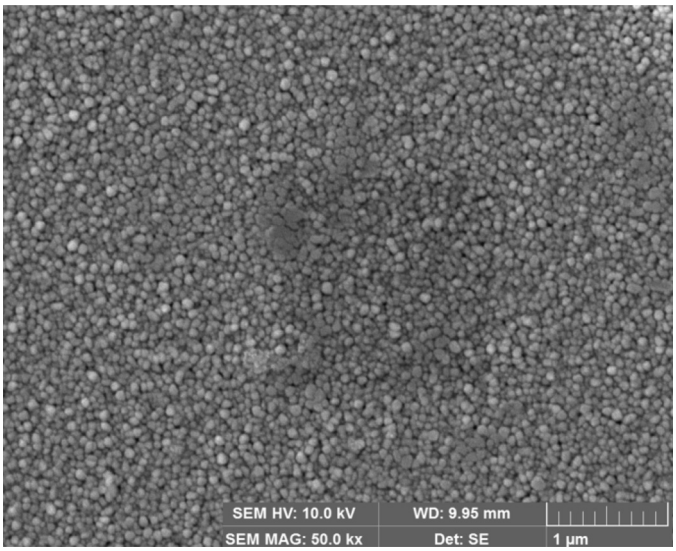

Fig. 2. SEM image showing grain structure of Au-covered surface.

2.7. Resonant frequency analysis

The resonant frequencies of the sensors were measured using a single pickup coil wound around a 250 μL Eppendorf tube, together with an Agilent® E5061B impedance analyzer. Sensors with dimensions 5 mm × 1 mm × 15 μm, covered or not with gold, were inserted into the tube with tube 200 μL of DMEM. The DC current furnished to the pickup coil was varied to maximize the signal received by the impedance analyzer. A measurement of the S_{11} parameter allowed the resonant frequency of the sensor to be determined. The resonant frequencies were measured for up to 70 h.

3. Results and discussion

The amorphous alloy Metglas® 2826MB3™ is an interesting sensor candidate given its large saturation magnetostriction, high magnetization, low anisotropy energy and low coercivity [28]. Recently, Holmes et al. studied the biocompatibility of a Metglas® 2826MB™ alloy and observed low compatibility in cell cultures [17]. Biological compatibility has been under study for magneto-elastic strips coated with materials that provide stability to the sensor system [12,23].

The thickness of the coating layer on a Si wafer placed next to the ME alloy surface during coating was evaluated by RBS analysis. RBS revealed values of Cr and Au of 128 nm and 117 nm, respectively (Fig. 1). In order to gain a perspective on these numbers, we note that the diffusion of Ni through Au films is a problem that has been studied in the area of microelectronics. The diffusion coefficient for Ni atoms through bulk Au is five orders of magnitude smaller than the grain boundary diffusion coefficient [29]. Abdul-Lettif [29] found that the grain boundary diffusion coefficient for Ni in Au is given by $D_b = (3 \times 10^{-4}\ cm^2/s)\ \exp(-0.94\ eV/kT)$. Therefore, even grain boundary diffusion is negligible at the temperatures of our experiments. Thus we do not expect atomic diffusion through grain boundaries in the Cr and Au films to occur in our experiments.

A typical spectrum is shown in Fig. 1 along with a simulation of that spectrum. By means of the simulation, RBS provides a non-destructive assessment of the quantitative concentration profiles of the elements down from the surface. The simulation shown in Fig. 1 assumed a Cr layer of 128 nm as well as an Au layer of 117 nm. The layers are seen to be well-defined, with little or no mixing. The determined thicknesses correspond to about 400–500 atomic diameters. Au-covered surfaces were further analyzed using SEM (Fig. 2), which showed a regular distribution of Au over the ribbon surface.

If the Mo and Ni ions cannot pass through the Au coating on the ME strips, then it is easy to understand the cytotoxicity results. Cytotoxicity assay with CHO cell lines was performed at different stages (1, 2 and 7 days) using the MTT method and showed significant reduction in cell survival after exposure to the strip not covered with gold (Fig. 3). This was not observed with the Au-coated strip compared to the control sample. Fig. 3 shows a decrease in the percentage of live cells compared to control over time for the uncoated strip, with a greater reduction after 7 days. However, strips covered with Au presented almost no statistical difference when compared with the control.

Degradation products present in the culture medium during cytotoxic analyses were determined over the course of one week (Table 1). The ion concentration of elements from the uncoated magneto-elastic alloy, after 7 days exposure, caused a ~50% reduction in cell survival. A similar time exposure of the Au-coated magneto-elastic alloy presented no reduction in cell survival.

In the present study, cyto-incompatibility of Metglas® 2826MB3™ induced a degradation process in living organ-

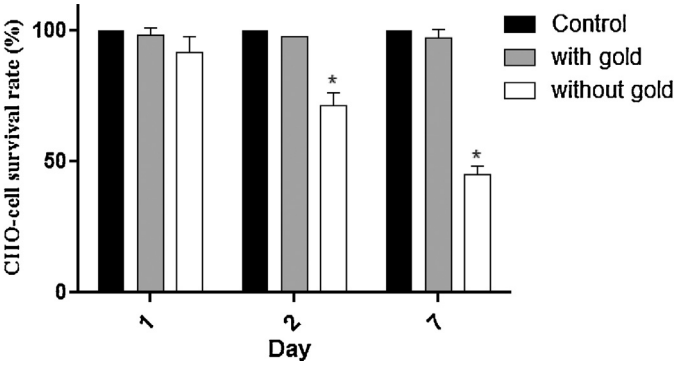

Fig. 3. Analysis of cell survival by MTT. Gold covered ME strip showed no significant difference in cell survival when compared to controls. However, a significant reduction in cell survival was observed in the uncoated strip from day 2. Results were obtained from three independent experiments. Bars with * correspond to statistically significant differences using ANOVA-Tukey test ($p \leq 0.05$) in comparison to control.

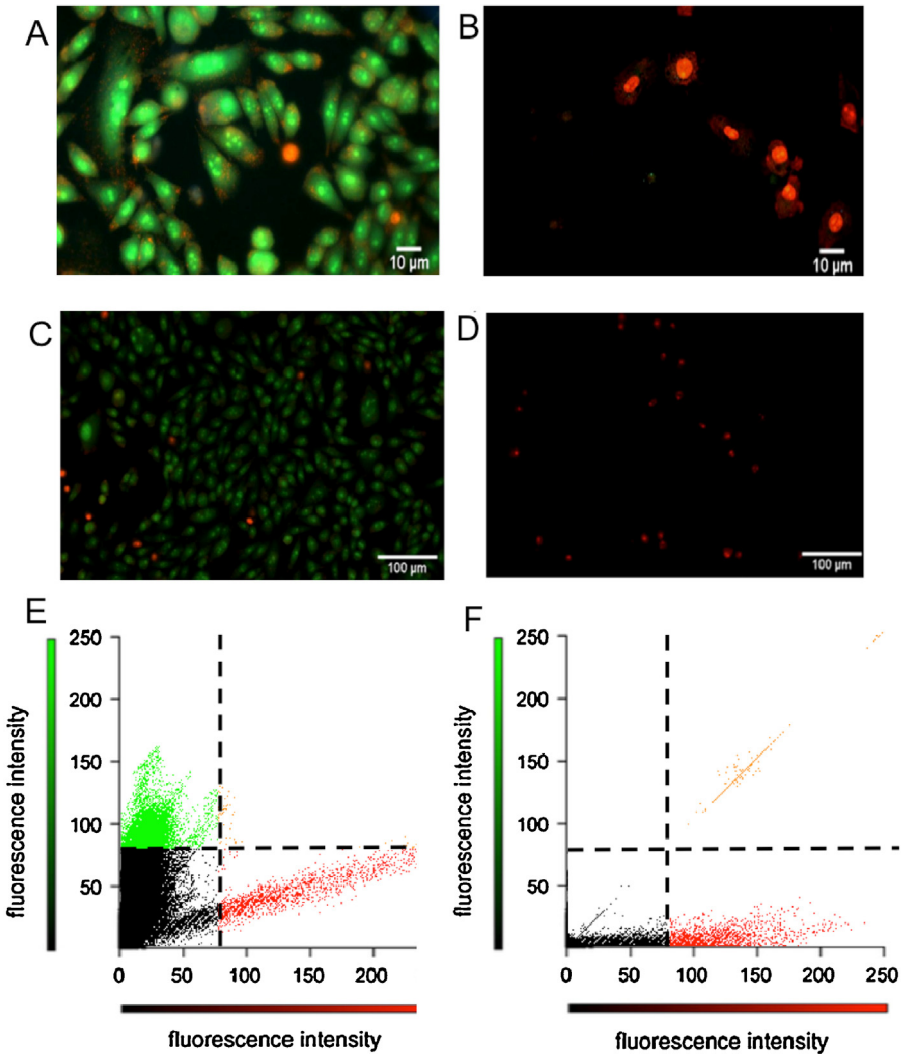

Fig. 4. *In situ* analysis of cell death through AO/EB staining: A and C—Au-covered strips with few cells stained by EB (red). Most of the cells presented normal morphology and were stained by AO (green). B and D—uncoated strips showing EB (red) staining indicating membrane permeability in dead cells. E—Correlation plot for the image presented in panel C. F—Correlation plot for the image presented in panel D. Dashed lines indicate thresholds of fluorescence at 75, taken from 8 bits extraction channel images chosen empirically, that separates visible fluorescence from dark pixels. No correlation was observed between images obtained in green and red spectral regions. Above these threshold pixel values, points were counted to evaluate the cell viability. The percentage of live cells was determined by dividing the number of green pixels by the total number of red and green pixels. Cell viability for image E presented 85.46% green in comparison to death morphology with 13.97% red and 0.57% yellow-orange fluorescence. No viable cells were observed in image F, corresponding to cells seen in panel D. Intensities from both green and red channels from below the threshold were not quantified and are represented in black. (For interpretation of the references to colour in this figure legend, the reader is referred to the web version of this article.)

Table 1
Degradation products present during cytotoxicity analyses were determined over the course of one week. The ion concentration in the culture medium after magneto-elastic alloy exposure was evaluated by Inductively Coupled Plasma-Optical Emission Spectrometry (ICP-OES) and is expressed in μg/mL.

Sample	Ion Concentrations (μg/mL)			
	Day 7			
	Fe	Ni	Mo	B
without Au	0.053	0.050	0.006	0.0066
with Au	0.000048	0.00005	0.0006	0.00026

isms, with the release of some of their atoms into the surrounding medium. This effect is related to degradation of the bare strip and the presence of metal atoms from the alloy, freely distributed in the culture medium [31–33]. The toxicity of these metal ions has been reported in different studies. Molybdenum has been associated with various toxic effects on the body, causing damage to various organs such as kidney, liver and spleen [18,19]. Furthermore, nickel was shown to be carcinogenic and toxic [20]. Taira et al. [21] demonstrated that nickel cytotoxicity shows a dose dependent pattern as released in media culture.

Induction of cell death was also evaluated through AO/EB *in situ* staining and showed significant reduction in cell survival and consequent low cell adhesion on top of ME strips not covered with Au, when compared to the Au-coated strip (Fig. 4). These results demonstrated the efficacy of working with ME sensors in conjunction with a gold coating to protect living cells. *In situ* analysis of samples not covered with gold showed a cell death pattern compatible with harmful cytotoxic effect (Fig. 4B and D) compared to the surface covered with gold (Fig. 4A and C). Gold coating protected cells, maintaining morphologically normal characteristics, with only a few cells presenting a pattern of cell death. Morphological cell patterns from the Au-coated surface were further analyzed through the ImageJ software in order to determine the number of normal cells and cells presenting death patterns. The dual AO/EB staining method generates color images, which were initially handled through channels. Normal cells presented a green fluorescence

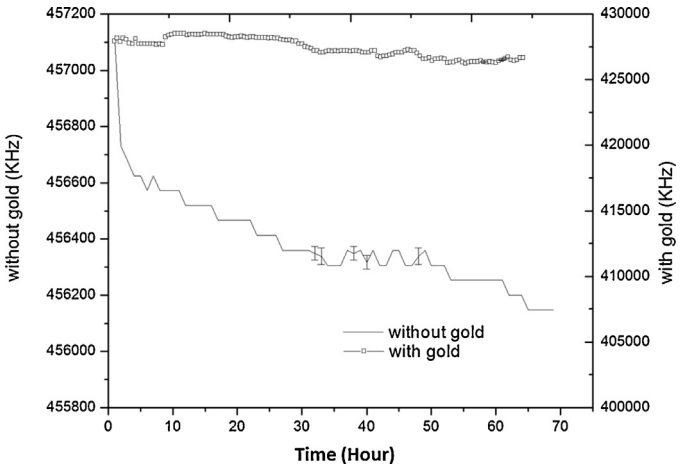

Fig. 5. Effect on the resonant frequency of the bare Metglas® 2826MB3™ ribbon compared to the Au-covered ribbon after 70 h exposure to the culture medium. Note frequency decrease in the first hours of experiment for bare ribbon.

(OA) in contrast with dead cells that present a red fluorescence (EB). The analysis of these result is presented in Fig. 4E. Most of the cells grown on top of the gold-covered sensor presented normal-like morphology represented by a green fluorescence (85.46%). The remaining cells show a death pattern and exhibit red and yellow-orange fluorescence (14.54%), with 13.97% red and 0.57% yellow-orange. No viable cells were observed in Fig. 4F, corresponding to cells seen in panel 4D.

Cytotoxicity of a biomaterial can be investigated using different types of cells for the MTT assay [34,35]. The MTT analysis as described by Denizot and Lang [24], measures mitochondrial activity of living cells and indirectly determines alterations in metabolic activity. The LIVE/DEAD assay is used to determine cellular membrane integrity since membrane-compromised cells are permeable to ethidium homodimer-1, which binds to nucleic acids resulting in nuclear-localized red fluorescence [36,37]. Several studies investigate biocompatibility of material surfaces in biomedical application by indirect analysis using the LIVE/DEAD assay [38–40]. Holmes et al. [36] studied the effect of cell cytotocixity on 2 types of ME materials, demonstrating qualitatively a lack of biocompatibility for the Metglas® 2826MB™ material.

Cell death can be classified according to its morphological appearance [41]. Two major cell death processes were considered here. Necrosis is morphologically characterized by a gain in cell volume, swelling of organelles, plasma membrane rupture and subsequent loss of intracellular contents. For a long time, necrosis has been considered merely as an accidental uncontrolled form of cell death. Apoptosis or programed cell death is characterized as a death pattern accompanied by rounding-up of the cell, with a progressive condensation of chromatin that induces nuclei to shrink into little single balls. In advanced stages of apoptosis, morphological changes characterized by nuclear and cytoplasmic condensation and cell fragmentation into membrane bound apoptotic bodies are observed [42,43]. Here, cells were grown on the top of the ME strips and analyzed trough AO/EB dual staining with discrimination of live from dead cells on the basis of membrane integrity. Degradation of the bare strip caused release of metal atoms from the alloy and induced cell death. Morphological cell changes could be easily observed from the monolayer of residual cells placed on sensor surfaces without gold protection. *In situ* analysis through AO/EB staining revealed red fluorescence from cells on top of the uncoated sensor, indicating that ethidium bromide (red) staining entered the cell because of membrane permeability. Cells presenting normal morphology, corresponding to most of those observed on the Au-covered strips, are stained only for acridine orange (green) staining, maintaining their membrane integrity. ImageJ analysis was performed and could find few cells with correlated pixels that looked yellow-orange, a condition also attributed to cell death. Cell viability for the Au-covered ME alloy presented 85.46% green fluorescence in comparison to the death morphologies on bare ME alloy with 13.97% red and 0.57% yellow-orange fluorescence.

Degradation of strips not covered with gold can be visualized by the instability of the resonance frequency, which is not seen on the alloy covered with gold, as reported in the present study. Effects on the resonant frequency of the bare Metglas® 2826MB3™ sensor are compared to those on the Au-covered sensor after 70 h exposure to the culture medium in Fig. 5. The resonant frequency of the bare sensor showed a much more expressive decrease indicating a net increase in mass, probably due to corrosion.

Exposing magneto-elastic material to a liquid medium may generate intermediate chemical reactions such as oxidation [44]. Iron corrosion may occur along with the leaching of other alloy components. The process of oxidation of metals has the characteristic formation of products such as oxides, which can adhere to the substrate base (magneto-elastic material) thereby increasing its mass. Another process that should be considered is the loss of alloy elements into the medium through leaching processes, causing changes in the characteristics and properties of the magneto-elastic material. The sum of these effects can be observed in the resonant frequency, which presents a marked decrease over time for the bare sensors, along with the amplitude of the signal response [2].

Coating surfaces of biosensors with gold layers is widely applicable because of their ability to form covalent bonds with spontaneous thiolates, facilitating bio functionalization via self-assembled monolayers (SAM) [45,46]. Huang et al. [23] observed qualitatively that coating Metglas® 2826MB™ ribbons with Au (thickness ~125 nm) maintains their physical properties and increases their stability. The gold and chromium coatings used in this study were found to have thicknesses of 117 nm and 128 nm through RBS. The biocompatibility of Metglas® 2826MB3™ strips was investigated here *quantitatively* through a survival assay in a cell culture. The results suggested that strips covered with gold presented an expressive reduction in cell death with an increase of cell surface adhesion. The percentage of living cells remained stable for different exposure times compared to the non-covered strip, where a decreased survival over time and a decreased adhesion of cells on the surface were observed.

Despite the good availability of Metglas® 2826MB3™, the resultant cytotoxicity from ion release should be carefully evaluated in each study design. Protection of alloys with appropriate coatings to ensure biocompatibility and avoid cytotoxicity has been explored [12]. The fact that the sensor is produced on a magneto-elastic substrate means that they have potential use in remote measurements for medical applications [47] and monitoring of different parameters in biological assays [11]. Gold is one of the most commonly used noble metal coating materials because of its high corrosion resistance, besides being very stable and inert. Another advantage of the gold coverage is the possibility of chemical functionalization with probes to recognize biomolecules. The present work has shown that the gold coating has the additional benefit of reducing cytotoxic effects due to ion release.

4. Conclusion

Wireless monitoring is an important plus when analyzing different biological processes. However, biological incompatibility of the magneto-elastic substrate alloy may induce cytotoxic processes due to the dissolution of Mo and Ni. Beside this, the ME sensor itself degrades in contact with the solutions, causing the experimental

results to be incorrectly interpreted. Applying coating materials like gold increases biocompatibility and the stability of magneto-elastic alloys, improving the final analysis. In this work, we have quantified the biological incompatibility in a particular case and have suggested a time scale for these effects. Experiments processed during seven days with the Cr/Au protective layer have shown very good signal stability of the sensor and high stability of the concentration of live cells, while, without the protective layer, during the same period, a reduction of 50% in the live cells was registered. Considering the huge variety of biological materials on numerous substrates that may interact and generate different biocompatibility issues, further studies are required to elucidate the effect of material degradation and potential effects generated after incubation in biological media.

Contributors

CM and MRE planned the experiments. ALP assisted with sample preparation. CM did the bulk of the data collection and MB assisted with data collection. ADS assisted with sample preparation and RBS analyses. STM analyzed the live/dead photographs. JAPH was responsible for MTT analyses. The paper was written by CM, MRE, and FPM, with input from all authors.

Funding

The funding sources had no role in the design of the study, in the collection or interpretation of the data, in the writing of the paper, or in the decision to submit the manuscript for publication.

Acknowledgments

This work was supported by Project 098412-7 from Fundação de Amparo à Pesquisa do Estado do Rio Grande do Sul (FAPERGS), Project 403-2500/12-5 from Secretaria de Desenvolvimento Econômico, Ciência e Tecnologia do Estado do Rio Grande do Sul (SDECT/RS) and Project 447777/2014-9 from Conselho Nacional de Desenvolvimento Científico e Tecnológico (CNPq). CM and MB were supported by fellowships from FAPERGS-CAPES, ALP was supported by a fellowship from CAPES, and FPM received partial support from CNPq. We acknowledge support from FINEP (contract 01.13.0359.00) and from Laboratório Central de Microscopia Prof. Israel Baumvol for the SEM analyses.

References

[1] C. Grimes, C. Mungle, K. Zeng, M. Jain, W. Dreschel, M. Paulose, K. Ong, Wireless magnetoelastic resonance sensors: a critical review, Sensors 2 (2002) 294.
[2] C.A. Grimes, S.C. Roy, S. Rani, Q. Cai, Theory, instrumentation and applications of magnetoelastic resonance sensors: a review, Sensors 11 (2011) 2809–2844.
[3] H. Lin, Z. Chen, Q. Lu, Q. Cai, C.A. Grimes, A wireless and sensitive sensing detection of polycyclic aromatic hydrocarbons using humic acid-coated magnetic Fe_3O_4 nanoparticles as signal-amplifying tags, Sens. Actuators B Chem. 146 (2010) 154–159.
[4] X. Gao, W. Yang, P. Pang, S. Liao, Q. Cai, K. Zeng, C.A. Grimes, A wireless magnetoelastic biosensor for rapid detection of glucose concentrations in urine samples, Sens. Actuators B Chem. 128 (2007) 161–167.
[5] X. Gao, R. Zhen, Y. Zhang, C.A. Grimes, Detecting penicillin in milk with a wireless magnetoelastic biosensor, Sensors Lett. 7 (2009) 6–10.
[6] S. Li, H.C. Wikle, B.A. Chin, High Throughput Screening for Food Safety Assessment, Woodhead Publishing, 2015.
[7] E.L. Tan, B.D. Pereles, B. Horton, R. Shao, M. Zourob, K.G. Ong, Implantable biosensors for real-time strain and pressure monitoring, Sensors 8 (2008) 6396–6406.
[8] E. Ghafar-Zadeh, Wireless integrated biosensors for point-of-care diagnostic applications, Sensors 15 (2015) 3236–3261.
[9] Y. Chai, H.C. Wikle, Z. Wang, S. Horikawa, S. Best, Z. Cheng, D.F. Dyer, B.A. Chin, Design of a surface-scanning coil detector for direct bacteria detection on food surfaces using a magnetoelastic biosensor, J. Appl. Phys. 114 (2013) 104–504.
[10] R. Guntupalli, R.S. Lakshmanan, J. Hu, T.S. Huang, J.M. Barbaree, V. Vodyanoy, B.A. Chin, Rapid and sensitive magnetoelastic biosensors for the detection of *Salmonella typhimurium* in a mixed microbial population, J. Microbiol. Methods 70 (2007) 112–118.
[11] X. Xiao, M. Guo, Q. Li, Q. Cai, S. Yao, C.A. Grimes, In-situ monitoring of breast cancer cell (MCF-7) growth and quantification of the cytotoxicity of anticancer drugs fluorouracil and cisplatin, Biosens. Bioelectron. 24 (2008) 247–252.
[12] H.R. Holmes, E.L. Tan, K.G. Ong, R.M. Rajachar, Fabrication of biocompatible vibrational magnetoelastic materials for controlling cellular adhesion, Biosensors 2 (2012) 57–69.
[13] A. Viswanath, S.R. Green, J. Kosel, Y.B. Gianchandani, Metglas–Elgiloy bi-layer, stent cell resonators for wireless monitoring of viscosity and mass loading, J. Micromech. Microeng. 23 (2013) 025010.
[14] Y. Jing, J. Liu, W.H. Ji, W. Wang, S.H. He, X.Z. Jiang, T. Wiedmann, C. Wang, J.P. Wang, Biocompatible Fe–Si nanoparticles with adjustable self-regulation of temperature for medical applications, ACS Appl. Mater. Interfaces 7 (2015) 12649–12654.
[15] P. Amrollahi, A. Ataie, A. Nozari, E. Seyedjafari, A. Shafiee, Cytotoxicity evaluation and magnetic characteristics of mechano-thermally synthesized CuNi nanoparticles for hyperthermia, J. Mater. Eng. Perform. 24 (2015) 1220–1225.
[16] B. Liu, T.F. Zhang, B.J. Wu, Y.X. Leng, N. Huang, In vitro cytocompatibility evaluation of hydrogenated and unhydrogenated carbon films, Surf. Coat. Technol. 258 (2014) 913–920.
[17] H.R. Holmes, A. DeRouin, S. Wright, T.M. Riedemann, T.A. Lograsso, R.M. Rajachar, K.G. Ong, Biodegradation and biocompatibility of mechanically active magnetoelastic materials, Smart. Mater. Struct. 23 (2014) 095036.
[18] G. Bompart, C. Pécher, D. Prévot, J.-P. Girolami, Mild renal failure induced by subchronic exposure to molybdenum: urinary kallikrein excretion as a marker of distal tubular effect, Toxicol. Lett. 52 (1990) 293–300.
[19] A. Vyskocil, C. Viau, Assessment of molybdenum toxicity in humans, J. Appl. Toxicol. 19 (1999) 185–192.
[20] Z. Zhang, P.Y.K. Chau, H.K. Lai, C.M. Wong, A review of effects of particulate matter-associated nickel and vanadium species on cardiovascular and respiratory systems, Int. J. Environ. Health Res. 19 (2009) 175–185.
[21] M. Taira, M.S. Toguchi, Y. Hamada, J. Takahashi, R. Itou, S. Toyosawa, N. Ijyuin, M. Okazaki, Studies on cytotoxic effect of nickel ions on three cultured fibroblasts, J. Mater. Sci. Mater. Med. 12 (2001) 373–376.
[22] M.A. Siddiqui, Q. Saquib, M. Ahamed, N.N. Farshori, J. Ahmad, R. Wahab, S.T. Khan, H.A. Alhadlaq, J. Musarrat, A.A. Al-Khedhairy, A.B. Pant, Molybdenum nanoparticles-induced cytotoxicity, oxidative stress G2/M arrest, and DNA damage in mouse skin fibroblast cells (L929), Coll. Surf. B: Biointerfaces 125 (2015) 73–81.
[23] S. Huang, J. Hu, J. Wan, M.L. Johnson, H. Shu, B.A. Chin, The effect of annealing and gold deposition on the performance of magnetoelastic biosensors, Mater. Sci. Eng. C 28 (2008) 380–386.
[24] F. Denizot, R. Lang, Rapid colorimetric assay for cell growth and survival. Modifications to the tetrazolium dye procedure giving improved sensitivity and reliability, J. Immunol. Methods 89 (1986) 271–277.
[25] L.R. Doolittle, Algorithms for the rapid simulation of Rutherford backscattering spectra, Nucl. Instrum. Methods Phys. Res. Sect. B 9 (1985) 344–351.
[26] W.-K. Chu, J.W. Mayer, M.-A. Nicolet, Backscattering Spectrometry, Academic Press, NY, 1978, pp. 89–122.
[27] E.V. Mironova, A.A. Evstratova, S.M. Antonov, A fluorescence vital assay for the recognition and quantification of excitotoxic cell death by necrosis and apoptosis using confocal microscopy on neurons in culture, J. Neurosci. Methods 163 (2007) 1–8.
[28] E. Hristoforou, Magnetostrictive delay lines: engineering theory and sensing applications, Meas. Sci. Technol. 14 (2003) R15.
[29] A.M. Abdul-Lettif, Grain boundary diffusion coefficients in gold–nickel thin films, Surf. Interface. Anal. 35 (2003) 429–431.
[30] A.L. Possan, C. Menti, M. Beltrami, A.D. Santos, M. Roesch-Ely, F.P. Missell, Effect of surface roughness on performance of magnetoelastic biosensors for the detection of Escherichia coli, Mater. Sci. Eng. C: Mater. Biol. Appl. 58 (2016) 541–547.
[31] D. Persaud-Sharma, N. Budiansky, *In vitro* degradation behavior of ternary Mg–Zn–Se and Mg–Zn–Cu alloys as biomaterials, J. Biomim. Biomater. Tissue. Eng. 18 (2013), http://dx.doi.org/10.4172/1662-100X.1000101.
[32] F.Y. Zhou, K.J. Qiu, H.F. Li, T. Huang, B.L. Wang, L. Li, Y.F. Zheng, Screening on binary Zr-1X (X = Ti, Nb, Mo, Cu, Au, Pd, Ag, Ru, Hf and Bi) alloys with good in vitro cytocompatibility and magnetic resonance imaging compatibility, Acta. Biomater. 9 (2013) 9578–9587.
[33] C.Y. Zheng, F.L. Nie, Y.F. Zheng, Y. Cheng, S.C. Wei, L. Ruan, R.Z. Valiev, Enhanced corrosion resistance and cellular behavior of ultrafine-grained biomedical NiTi alloy with a novel SrO–SiO_2–TiO_2 sol–gel coating, Appl. Surf. Sci. 257 (2011) 5913–5918.
[34] Z. Zhou, X. Liu, Q. Liu, L. Liu, Evaluation of the potential cytotoxicity of metals associated with implanted biomaterials (I), Prep. Biochem. Biotechnol. 39 (2009) 81–91.
[35] Y. Yang, J. Nan, J. Hou, B. Yu, T. Zhao, S. Xu, S. Lv, H. Zhang, Cytotoxicity of gold nanoclusters in human liver cancer cells, Int. J. Nanomed. 9 (2014) 5441–5448.
[36] H.R. Holmes, A. DeRouin, S. Wright, T.M. Riedemann, T.A. Lograsso, R.M. Rajachar, K.G. Ong, Biodegradation and biocompatibility of mechanically active magnetoelastic materials, Smart. Mater. Struct. 23 (2014) 095036.
[37] I. Gherghi, S.T. Girousi, A.N. Voulgaropoulos, R. Tzimou-Tsitouridou, Study of interactions between DNA-ethidium bromide (EB) and DNA-acridine orange

(AO), in solution, using hanging mercury drop electrode (HMDE), Talanta 61 (2003) 103–112.
[38] M. Schinhammer, I. Gerber, A.C. Hanzi, P.J. Uggowitzer, On the cytocompatibility of biodegradable Fe-based alloys, Mater. Sci. Eng. C: Mater. Biol. Appl. 33 (2013) 782–789.
[39] C.M. Haslauer, J.C. Springer, O.L. Harrysson, E.G. Loboa, N.A. Monteiro-Riviere, D.J. Marcellin-Little, In vitro biocompatibility of titanium alloy discs made using direct metal fabrication, Med. Eng. Phys. 32 (2010) 645–652.
[40] M. Bhuyan, J. Rodriguez-Devora, K. Fraser, T.-L. Tseng, Silicon substrate as a novel cell culture device for myoblast cells, J. Biomed. Sci. 21 (2014) 47.
[41] W. Malorni, G. Donelli, Cell death. General features and morphological aspects, Ann. N. Y. Acad. Sci. 663 (1992) 218–233.
[42] G. Kroemer, L. Galluzzi, P. Vandenabeele, J. Abrams, E.S. Alnemri, E.H. Baehrecke, M.V. Blagosklonny, W.S. El-Deiry, P. Golstein, D.R. Green, M. Hengartner, R.A. Knight, S. Kumar, S.A. Lipton, W. Malorni, G. Nunez, M.E. Peter, J. Tschopp, J. Yuan, M. Piacentini, B. Zhivotovsky, G. Melino, Nomenclature committee on cell, classification of cell death: recommendations of the nomenclature committee on cell death, Cell. Death. Differ. 16 (2009) 3–11.
[43] A.H. Wyllie, G.J. Beattie, A.D. Hargreaves, Chromatin changes in apoptosis, Histochem. J. 13 (1981) 681–692.
[44] D. Landolt, Corrosion and Surface Chemistry of Metals, EPFL, Press, Lausanne Switzerland, 2007.
[45] G. Thakur, K. Prashanthi, T. Thundat, Directed self-assembly of proteins into discrete radial patterns, Sci. Rep. 3 (2013) 1923.
[46] M.Y. Mulla, E. Tuccori, M. Magliulo, G. Lattanzi, G. Palazzo, K. Persaud, L. Torsi, Capacitance-modulated transistor detects odorant binding protein chiral interactions, Nat. Commun. 6 (2015), http://dx.doi.org/10.1038/ncomms7010.
[47] H. Holmes, E.L. Tan, K.G. Ong, R.M. Rajachar, Real-time, in vivo investigation of mechanical stimulus on cells with remotely activated, vibrational magnetoelastic layers, Conf. Proc. IEEE. Eng. Med. Biol. Soc. (2011) 3979–3982.